Sm–Nd and Sr isotope systematics of scheelite from the giant Au(–W) deposit Muruntau (Uzbekistan): Implications for the age and sources of Au mineralization

Article *in* Mineralium Deposita · August 2001

DOI: 10.1007/s001260100156

5 authors, including:

B. V. Belyatsky
All-Russian Geological Institute, St-Petersburg, Russia

Robert Krymsky
A.P. Karpinsky Russian Geological Research Institute

Mineralium Deposita (2001) 36: 379–392
DOI 10.1007/s001260100156

ARTICLE

U. Kempe · B.V. Belyatsky · R.S. Krymsky
A.A. Kremenetsky · P.A. Ivanov

Sm–Nd and Sr isotope systematics of scheelite from the giant Au(–W) deposit Muruntau (Uzbekistan): implications for the age and sources of Au mineralization

Received: 14 March 2000 / Accepted: 19 December 2000 / Published online: 11 May 2001

Abstract The application of the Sm–Nd isotope system of scheelite to dating of low-sulfide, quartz-vein hosted Au mineralization is still under discussion. In the present work, new Sm–Nd and Rb–Sr data for scheelite from the giant Muruntau/Myutenbai Au deposit (Kyzylkum, Western Uzbekistan) are discussed. Based on the geological relationship, mineralogical properties, and trace element characteristics, two types of scheelite can be distinguished within the deposit. The first one is represented by early bluish luminescent and weakly coloured scheelite (generation 1) found within strongly deformed flat quartz veins. The apparent isochron defined by this scheelite (351 ± 22 Ma) is interpreted as a mixing line. Typically brownish to orange and yellowish luminescent scheelite from steeply dipping veins (generation 2) defines a Sm–Nd isochron age of 279 ± 18 Ma ($\epsilon_{Nd} = -9.5 \pm 0.3$; MSWD: 1.5). No evidence for mixing or disturbance by late alteration were found for these scheelites. This Sm–Nd isochron age agrees with the Rb–Sr and K–Ar age range for wall rock alteration in this deposit reported previously. The age of 280 Ma is interpreted to date the high-grade ore formation in the Muruntau deposit. There are currently no reliable age data available on the magmatic events in the Muruntau region. Probably, there is some overlap in time of the Hercynian gold deposition with the intrusion of lamprophyric dykes. The Nd and Sr isotopic signatures of scheelite define the wall rocks (mainly metasiltstones and metasandstones) as the most probable sources for these elements in scheelite.

Editorial handling: H.E. Frimmel
P.A. Ivanov deceased

U. Kempe (✉)
Institute of Mineralogy,
Freiberg University of Mining and Technology,
Brennhausgasse 14, 09596 Freiberg, Germany
E-mail: kempe@orion.hrz.tu-freiberg.de

B.V. Belyatsky · R.S. Krymsky
Institute of Precambrian Geology and Geochronology,
Russian Academy of Sciences, Makarova emb. 2,
199034 St. Petersburg, Russia

A.A. Kremenetsky
Institute of Mineralogy, Geochemistry, and Crystallochemistry
of Rare Elements, Russian Academy of Sciences,
ul. Veresaeva 15, 121357 Moscow, Russia

P.A. Ivanov
Institute of Geology of Ore Deposits, Moscow State Academy
of Geological Exploration, ul. Miklukha Maklaya 23,
117485 Moscow, Russia

Introduction

The direct age determination of low-sulfide quartz-vein hosted Au mineralization is usually hampered for several reasons. Quite often, reliable conventional isotope systems directly related to Au mineralization are not available (e.g. U–Pb in zircon) or disturbed by late alteration processes (e.g. K–Ar and Rb–Sr in mica). Relative age relations between Au deposition and magmatic or metamorphic events as well as formation of hydrothermal mineral associations is difficult to establish only by field observations. Moreover, detailed petrographic work is necessary in most cases to distinguish between wall rock alteration caused by metamorphism and hydrothermal alteration respectively. As a result, genesis and timing of Au mineralization remain controversial for several world-class deposits (Kerrich 1991; Frei et al. 1998).

In the last few decades, the Sm–Nd isotope method has been introduced for direct age and source determinations in U deposits (Fryer and Taylor 1984), Pb–Zn deposits (Halliday et al. 1990; Chesley et al. 1991), and Sn–W deposits (Belyatsky et al. 1992; Belyatsky et al. 1994; Kempe and Belyatsky 1994; Li et al. 1994; Krymsky et al. 1995). For isotope dating, the Sm–Nd system in vein minerals (e.g. uraninite, scheelite, wolframite, and fluorite) containing considerable amounts of rare earth elements was used.

Mineralogical as well as trace element studies on scheelite from Au deposits suggest simultaneous formation of scheelite with native Au and show that, in general, the mineral is suitable for Sm–Nd age determination (Anglin et al. 1987; Mueller et al. 1991; Kempe and Oberthür 1997). But the first Sm–Nd age data reported by Bell et al. (1989) for scheelite from Au deposits in the Timmins area (Canada) apparently yielded an age roughly 200 Ma younger than other methods. Scheelite used for isotope investigations was sampled from different deposits and from various geological settings. Up to now, the age determined by Bell et al. (1989) using the scheelite Sm–Nd isochron method remains equivocal (for discussion see e.g. Spooner 1991; Corfu 1993; Anglin et al. 1996; Frei et al. 1998). Anglin (1990) reported preliminary Sm–Nd scheelite ages for the Val d'Or Au deposits (Quebec, Canada) coinciding with Ar–Ar muscovite-Cr (fuchsite) and U–Pb rutile ages for the same deposits. However, these results were thought to be not related to the Au deposition but to a later alteration event (e.g. Spooner 1991). Nevertheless, further investigations on scheelite and tourmaline from the Val d'Or deposits by Anglin et al. (1996) indicated that Sm–Nd isochron ages for scheelites probably reflect the time of Au deposition which was found to be 60–70 Ma younger than any magmatic or metamorphic activity in the region.

Kent et al. (1995) obtained a Sm–Nd errorchron (MSWD = 13.9) for six scheelite samples from the Mount Charlotte mine (Western Australia) defining an age that was 170 Ma older than the Ar–Ar muscovite age. The linear array in the Sm–Nd isotope plot was interpreted to represent a mixing line (Kent et al. 1995). However, extremely high ϵ_{Nd} values (3.5–9.0) were calculated for scheelites at the time assumed to be the age of Au mineralization. It was argued that these unusual ϵ_{Nd} values indicate a genetic relationship between the Au mineralization and komatiites present in the same region. Komatiites were discussed as a source of Nd and Au, although the Nd contents in these rocks are extremely low (1–2 ppm) and some ϵ_{Nd} values calculated for scheelite samples are significantly higher than for komatiites or for any other rock in the region.

Darbyshire et al. (1996) reported three Sm–Nd isochrons for 25 scheelite samples from 19 different gold deposits in the Archean Midlands greenstone belt (Zimbabwe). Two mineralization events (Late Archean and Early Proterozoic) were distinguished by the Sm–Nd isochron method.

In general, it remains unclear from this short review whether the Sm–Nd isochron method on scheelite is suitable to date Au mineralization and to constrain the fluid sources (in combination with a discussion of the Sr isotope ratios of the same samples) or not. We point out that all examples reported in the literature concern Archean or Proterozoic Au mineralization in greenstone belts. The paragenetic position of scheelite in these deposits is often not well defined.

In this work, we present mineralogical as well as Sm–Nd and Rb–Sr isotope data for 12 scheelite samples from the giant Muruntau/Myutenbai Au deposit (Uzbekistan). Additionally, one sample from the nearby Au–Ag deposit at Kosmanachi was investigated. In contrast to Au deposits in Ontario/Canada, Western Australia, and Zimbabwe, the Muruntau deposit is hosted by Paleozoic rocks and not related to a greenstone belt. Nevertheless, the style of the Au mineralization is similar to the deposits mentioned above.

Geological and geochronological data published mainly in the Russian literature and constraining the age and the genesis of the Muruntau deposit are briefly summarized here because many data are not easily accessible to the English reader.

Geological setting and sampling strategy

The giant Muruntau Au(–W) deposit with > 3,400 t of Au (1,186 t of Au were recovered in 1967–1995; 2,230 t of Au were estimated as proven reserves in 1995), the largest recently known individual Au deposit (cf. Drew et al. 1996; Shayakubov et al. 1999), was discovered by Soviet geologists in 1958. Despite a large number of publications from Uzbekistan, Russian, and (in recent years) American workers, several problems of geology, stratigraphy, magmatism, and hydrothermal activity in the vicinity of the Muruntau Au(–W) deposit as well as of the age and genesis of the Au(–W) mineralization are still unresolved. However, the geological setting of the mineralization yields some important constraints on the interpretation of both the age and the mechanisms of ore formation. The following short résumé is based on literature data in combination with our own field observations.

The Muruntau deposit is located in the Central Kyzylkum desert, Western Uzbekistan (Fig. 1) to the south of a suture line separating the Central Kazakhstan–North Tien Shan continent to the north-east from the Kara Kum massif to the south-west (Drew et al. 1996). In this area, several Au(–Ag–W) deposits were found inside Caledonian to Hercynian tectonic windows of the folded basement in Meso-Cenozoic platform sediments (Fig. 1; cf. Kraft and Kampe 1994). In the Muruntau region, the metamorphic rocks are strongly dislocated and were traditionally subdivided into two units: (1) schists with some layers of mafic metavolcanics and carbonaceous rocks belonging to the so-called Taskazgan suite and (2) intercalations of metasiltstones, metasandstones, and schists with interbeds of gritstone, limestone, and cherts of the Besapan suite hosting the Muruntau deposit (Fig. 2). These rocks are metamorphosed in lower greenschist (Besapan) to lower amphibolite facies (Taskazgan). Inside the Tamdytau tectonic window, the rocks of the two suites were overthrust by Devonian and Carboniferous dolomitic marbles to the north and north-east of the Muruntau deposit (Fig. 2). While the biostratigraphic age of the marbles is well established (cf. Kostitsyn 1996), the age of the Taskazgan and Besapan suites is still controversial (e.g. Akhmedzhanov et al. 1979; Bukharin et al.

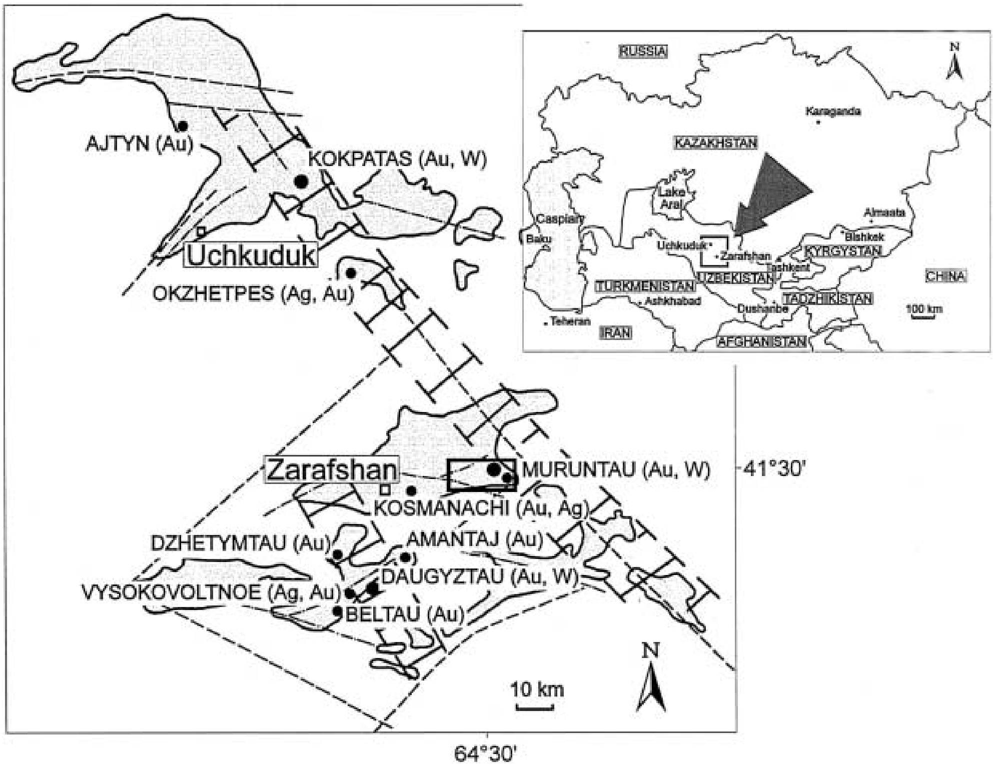

Fig. 1 Location of the Muruntau and other Au deposits within the Paleozoic tectonic windows (*shaded areas*) in the platform sediments (*white areas*) of the Central Kyzylkum desert (Uzbekistan). Large faults are shown as *dashed lines*, axis of large anticline structures as *dot–dashed lines*, and syncline structures as *"ladders"*. The towns of Uchkuduk and Zarafshan are also given. The *rectangle* indicates the location of Fig. 2

1984; Mukhin et al. 1988; Drew et al. 1996). The Besapan suite is usually subdivided into four subsuites, according to colour in outcrops: Grey Besapan Bs_1, Black Besapan Bs_2, Variegated Besapan Bs_3, and Green Besapan Bs_4 respectively; the Grey and the Black Besapan units are often considered as a single unit (cf. Fig. 2). The Bs_1 and Bs_2 were found to be Ordovician (O_{2+3}), the Bs_3 to have an Ordovician to Silurian age (O_3–S_1), and the Bs_4 was assigned to the Silurian (S_1). The fossil content of the Variegated Besapan Bs_3 indicates a tectonic mixture (Bukharin et al. 1984). Mukhin et al. (1988) reinterpreted the metamorphic rock unit in the Tamdytau window as a stack of nappes and the Variegated Besapan as a tectonic lens ("Muruntau lens") separated from the hanging wall and the footwall by blastomylonites (ϵ_2–O_2 for Bs_1 and Bs_3, whereas Bs_2 and Bs_4 were considered to be O_2–S_1). Au mineralization occurs only inside the Variegated Besapan unit in the Muruntau area.

Additional constraints on the age of the Au mineralization at Muruntau stem from the occurrence of "conglomerates" at the footwall of the Devonian marbles. These "conglomerates" contain Au-bearing vein quartz and granite pebbles indicating a Caledonian age (or event) of the Au mineralization (upper age limit: D_1) if these rocks are interpreted as a basal conglomerate (Askarov and Bigaeva 1965; Gar'kovec 1971, 1973; Rakhmatullaev 1980). Nevertheless, a detailed investigation by Kotov and Poritskaya (1991) appeared to prove a tectonic formation of these pseudoconglomerates which most probably post-date all Caledonian events.

Although Hercynian granites are discussed as a possible source for Au mineralization, there are no specific studies dealing with the relationships between granitic rocks and the ore formation. The only magmatic rocks exposed in the area of the Muruntau deposit are dykes arranged into three chains (Fig. 2). To the south and to the north of the Muruntau deposit, alkaline dykes (including kersantite and alkaline granites) occur, whereas the dyke swarm cross-cutting the Muruntau deposit consists of altered granites and granodiorites (cf. Kostitsyn 1996). A larger granite body (the so-called Sardarin pluton) was found roughly 15 km to the south-east of Muruntau under the platform sediments. Another granite (the so-called Murun granite) was discovered by deep drilling (SG-10) at a depth interval from 4005 m to the bottom of the hole at 4294 m. Granites also outcrop in the Tamdytau mountains to the north and in the Aristantau mountains to the south of Muruntau.

The Muruntau deposit may be interpreted as a typical shear-zone related, Au-bearing quartz-vein system. There are two principal quartz-vein systems – one of so-called flat veins, that are shallow dipping, strongly deformed, boudinaged, clearly affected by thrusting and low-grade in Au, and another of "central" and "stockwork" veins, which are steeply dipping, brecciated, only slightly deformed, and high-grade in gold. Later veinlets of sulfide, tourmaline, quartz–feldspar, and carbonate types are of minor importance (e.g. Zarembo 1968; Rakhmatullaev 1980; Uspenskiy and Aleshin 1993; Berger et al. 1994; Kostitsyn 1996). The steep vein system clearly cross-cuts and displaces early flat structures (cf. the contour of ore-bearing metasomatically altered

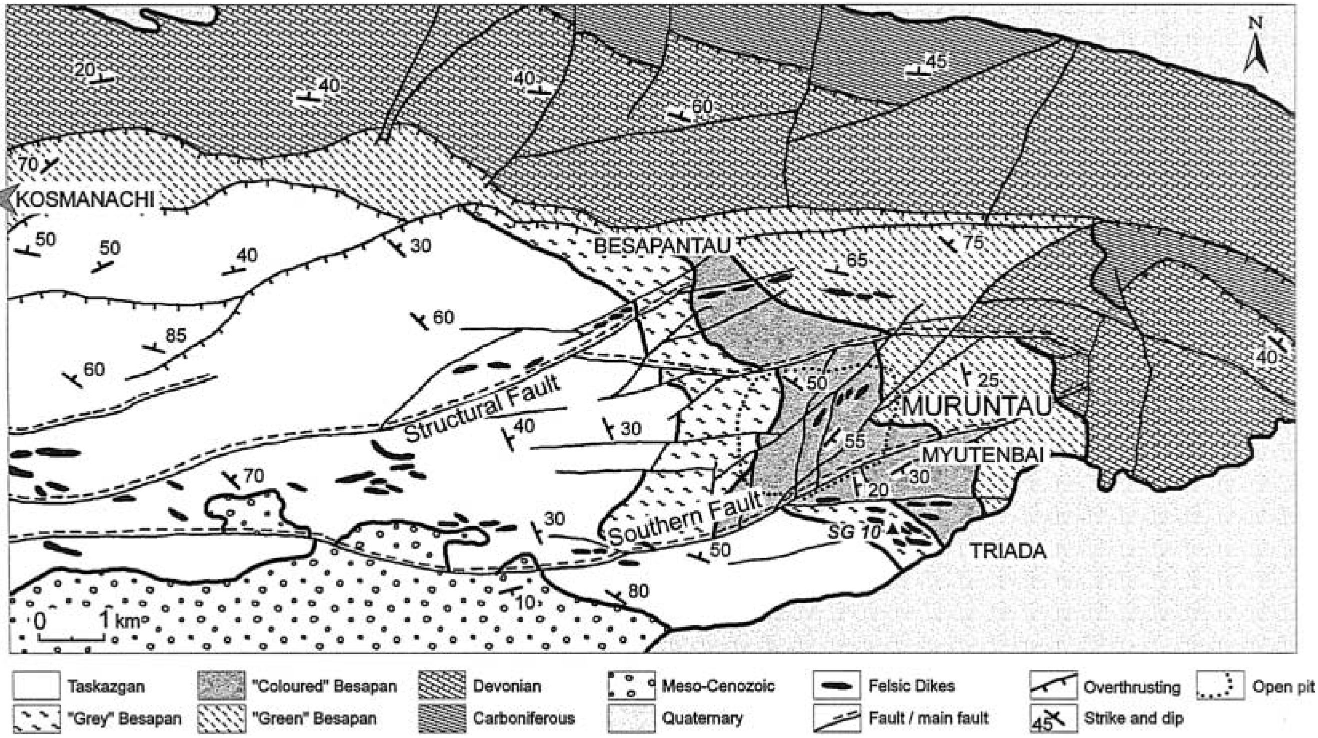

Fig. 2 Geological sketch of the Muruntau ore field. Location of the Au–Ag deposit Kosmanachi (sample KM 80–532) is roughly 3 km to the west from the left border of the sketch within the Variegated Besapan. Terminology given here for rock/stratigraphic units is consistent with the one used by local geologists (cf. Drew et al. 1996, see text for further explanation). The location of deep drill hole SG 10 is given by the *black triangle*

rocks in Fig. 3). Drew et al. (1996) assumed that the schistosity and thrusting structures within the Besapan suite were formed during the Caledonian tectonism. Au deposition took place during the Hercynian tectonic cycle (Carboniferous to Permian) starting from the reactivation of Caledonian tectonic structures within the left-lateral Sangruntau–Tamdytau shear zone (i.e. within the "Muruntau lens") with formation of an "initial" Au mineralization. In continuation of this process, according to these authors, brittle–ductile deformation led to folding of the Besapan unit and to activation of the large left-lateral Muruntau–Daughyztau shear zone with the formation of high-grade Au ores in steeply dipping vein systems and with simultaneous intrusion of granitic plutons.

Low-grade ore bodies are nearly horizontal and stratiform (Savchuk et al. 1987). In contrast, high-grade ore bodies are steeply dipping and cone-shaped (cf. Shayakubov et al. 1999). The innermost parts of these bodies consist of single, "central" veins that are quartz bodies with strong brecciation features, especially at the vein walls. Outer parts of the "cones" were formed by stockwork veins. As can be seen in Fig. 2, formation of these vein systems was controlled by brittle deformation within the "Muruntau lens" accompanying shearing along large faults to the north and the south of the Muruntau deposit.

There has been a continual discussion on the genesis of the Muruntau deposit. In early works, but also in some recent publications, Au mineralization was seen as being related to Hercynian granite magmatism (e.g. Khamrabaev 1958; Kostitsyn 1996). Later, the theory of a syngenetic (black-shale type) and/or metamorphic (Caledonian) formation of the ores was extensively discussed in the literature (e.g. Petrovskaya 1968; Bel'kova and Ognev 1971; Gar'kovec 1973, 1975; Voronkov 1976; Savchuk et al. 1987; Mukhin et al. 1988; Procenko 1990; Procenko and Rubanov 1991; Bojcov et al. 1996). In some recent papers, the involvement of mantle-related sources was discussed (Kotov and Poritskaya 1991; Marakushev and Khokhlov 1992).

Several authors assumed a coincidental association of Au and W mineralization formed at different times and resulting from different ore-forming processes (e.g. Badalova and Palej 1965; Petrovskaya 1968; Vikhter et al. 1986). In other publications, a genetic link between the precipitation of native gold and the occurrence of scheelite was suggested (e.g. Procenko and Rubanov 1991). Uspenskiy and Aleshin (1993) found that in stratiform scheelite ore bodies, scheelite does not show any clear association with gold. In contrast, a close Au–W association was found near and within the steeply dipping "central" veins. Uspenskiy and Aleshin (1993) distinguished three scheelite generations according to their mineral associations: (1) pyroxene–amphibole–quartz; (2) gold–sulfide–quartz; (3) tourmaline–sulfide–quartz. According to our data (see Table 1), at least two scheelite types may be distinguished according

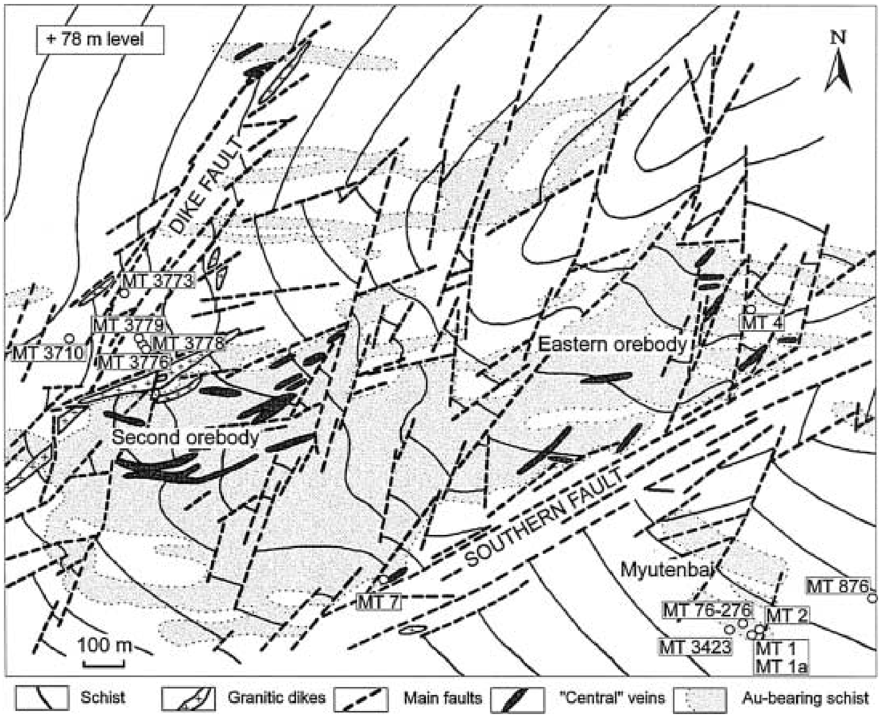

Fig. 3 Geological sketch of the +78 m level of the Muruntau/Myutenbai underground mine with sample locations. Sample MT 7 is projected from the +410 m level of the Muruntau open pit. Samples MT 76–276, MT 876, and MT 3423 are projected from the +220 m level of the Myutenbai mine

Table 1 Mineralogical properties, trace element, and isotope characteristics of scheelite 1 and 2 from the Muruntau Au deposit

	Scheelite 1	Scheelite 2
Geological position	In flat veins or in metasomatites parallel to the foliation	In steeply dipping veins crosscutting the foliation
Mineral association	Greyish quartz, pyrite, pyrrhotite, K-feldspar, chlorite, apatite, calcite	White quartz, sericite, carbonates, pyrite, molybdenite
	Intergrowths with sulfides common	Intergrowths with sulfides not common
	Low-grade Au	High-grade Au
Mineral properties		
Shape	Strongly deformed, disseminated grains, seldom aggregates up to 1-2 cm in diameter	Aggregates of zoned, brecciated crystals up to a few centimetres in diameter
Color	Brownish-grey to white	Brownish-yellow to orange
Luminescence	Strong bluish-white	Quenched yellowish
Trace elements		
Sr	200–260 ppm	400–1100 ppm
La	15–140 ppm	15-80 ppm
Ce	30–250 ppm	60-350 ppm
Nd	30–60 ppm	65–250 ppm
Sm	5–15 ppm	20–90 ppm
Eu	2–7 ppm	9–130 ppm
Tb	1–3 ppm	3–75 ppm
Lu	0.5–4 ppm	0.2–3 ppm
Isotope ratios		
$^{87}Sr/^{86}Sr$	0.7147–0.7151	0.7147–0.7156
$^{143}Nd/^{144}Nd$	0.51196–0.51208	0.51206–0.51234

to their location (Kempe and Oberthür 1997; Kempe et al. 1999). Scheelite 1 occurs in flat veins and adjacent rocks (similar to scheelite 1 from Uspenskiy and Aleshin 1993) and scheelite 2 may be found in steeply dipping veins and stockworks (mainly scheelite 2 from Uspenskiy and Aleshin 1993). For mineralogical and isotope investigation, five samples of scheelite 1 from Muruntau and eight samples of scheelite 2 from Muruntau, Myutenbai, and Kosmanachi were selected (cf. Figs. 2 and 3).

Previous geochronological work

In comparison with other large Au deposits, absolute age data concerning the Muruntau ore deposit are rare. Earlier K–Ar dating of magmatic rocks yielded a large scatter of ages from 160 to 580 Ma (Askarov and Bigaeva 1965; Palej and Sher 1970; Rakhmatullaev 1980; Kostitsyn 1991). Askarov and Bigaeva (1965) concluded that the main granite magmatism in the Kyzylkum may be dated at 260–270 Ma and that there were one younger (250 Ma) and several older (310; 360–370; and 460 Ma) magmatic events. Rakhmatullaev (1980) suggested an age of around 265–277 Ma for early metasomatic alteration and "central", steeply dipping quartz veins in Muruntau, and around 250–260 Ma for late dykes and sulfide veins.

Selected K–Ar age data from the literature for biotite, amphibole, and microcline were recalculated using recently accepted decay constants (see Table 2). An age around 275 Ma was obtained for the potassic wall rock alteration (secondary biotite and feldspar) as well as for the intrusion of lamprophyric dykes, and ages of around 240–250 Ma were calculated for late quartz–adularia veins containing Au–Ag mineralization (cf. Table 2).

Table 2 Summary of absolute age data on the Muruntau Au deposit. *Bold* Event at 270–280 Ma; *italics* altered samples; *WR* whole rock; *Adu* adularia; *Amf* amphibole; *Bt* biotite; *Ksp* K-feldspar; *Mi* microcline; *Ser* sericite

	K-Ar (biotite, sericite, K-feldspar, and amphibole)	Rb-Sr ("quasi-mineral" isochrons)	Sm-Nd (scheelite isochrons)
Wall rock metamorphism		403±18 Ma[a] 393±26 Ma[a]	
Flat quartz veins			351±22 Ma[b] ("mixing line")
Effusives (D-C)			
Basalt	302± 8 Ma; Amf[c]		
Biotite granite	264±6 Ma; Bt[c]	286± 2 Ma[d] 287±39 Ma[a] *255±15 Ma; Fsp*[a]	
Granodioritic Dike		284± 2 Ma[d]	
Alkaline dikes			
Syenite	*256±11 Ma;* Mi[e] *248± 3 Ma;* Amf[f] *239± 3 Ma;* Amf[f]	**274± 6** Ma[d]	
Lamprophyre	**277±5** Ma ?[g]	**274± 5** Ma[d]	
Metasomatites			
Biotitization ("hornfelses")	**275±9** Ma; Bt[e] **271±9** Ma; Amf[f] **277±5** Ma; Bt[h]	**273± 3** Ma[d]	
Feldspatization	**274±13** Ma; Mi[e]	**271±17** Ma[d]	
Quartz zones ("central veins")			**279±18** Ma[b]
Arsenopyrite-quartz veins		230± 4 Ma[d]	
Late adularia-quartz veins	242±10 Ma; Adu[e] 247± 5 Ma; Adu[f] 224±10 Ma; Ser[j]	237± 4 Ma[i]	

[a]Kostitsyn (1996): Black Besapan – Tamdytau, borehole S260; Green Besapan – Amantaj, borehole S6012; Murun granite – superdeep drilling SG 10, WR isochrone and feldspar isochron
[b]This study
[c]Askarov and Bigaeva (1965): basalt – Tamdytau Mts.; biotite granite – Tamdytau intrusion (average; $n = 5$)
[d]Kostitsyn (1991): biotite granite – drilling 15 km south-east of the ore field; granodiorite dyke – Muruntau mine; syenite dyke – superdeep drilling SG 10; lamprophyre – Mt. Tamdytau, north of Muruntau; "hornfels" – Muruntau mine; feldspatite – Muruntau mine (other samples: feldspatite 272 ± 9 Ma, MSWD 6.4; sericite metasomatite (fraction without sericite, Au 0.3 ppm) 274 ± 8 Ma, MSWD 1.8; sericite metasomatite (fraction with sericite, Au 60 ppm) 255 ± 10 Ma, MSWD 1.4; tourmalinite 257 ± 13 Ma, MSWD 4.6)
[e]Palej and Sher (1970): syenite, altered – trench; "hornfels"- trench; quartz–microcline metasomatite; quartz–adularia vein (all Muruntau)
[f]Rakhmatullaev (1980): syenite, altered; "hornfels"; quartz–adularia vein
[g]Kremenetsky et al. (1990): lamprophyre
[h]Fuks and Rublev in Kostitsyn (1996): "hornfels"-superdeep drilling SG 10
[i]Kostitsyn and Rusinova (1987): quartz-adularia vein
[j]Kostitsyn (1993): quartz-adularia vein-Muruntau mine

Extensive studies on the Rb–Sr isotope systems of metamorphic rocks, magmatic rocks, and metasomatically altered rocks, as well as of veins and minerals were carried out by Kostitsyn and co-workers by the use of density fractions of single rock samples (i.e. "quasi-mineral" isochrons; Kostitsyn and Rusinova 1987; Kostitsyn 1991, 1993, 1994, 1996; Koltsov and Kostitsyn 1995). According to these authors, the metamorphism of the host rocks in the Muruntau region took place at 400 Ma. In Hercynian time, two magmatic events were distinguished. The intrusion of "normal" granites (Murun, Sardarin, some granitic dykes) was dated at 286 Ma (Table 2). The emplacement of alkaline dykes (kersantite, alkaline granite) overlaps in time with the formation of the ore-bearing metasomatically altered rocks at 273 Ma. Kostitsyn (1996) also suggested three later events: (1) metamorphism in the Taskazkan suite, deformation of the Murun granite, and formation of quartz–tourmaline veins and breccias (258 Ma); (2) formation of quartz–arsenopyrite veinlets (230 Ma); and (3) formation of late Ag–Au quartz–adularia veins (219 Ma, Table 2). There are no indications for external input of Sr from outside of the Besapan suite according to the investigations by Kostitsyn and co-workers. Nevertheless, a transport of Au and W from external (deep-seated) sources was not excluded in recent publications (Kostitsyn 1996).

Methods

The investigation of vein samples and thin sections containing scheelite using a binocular microscope, luminescent lamp (long- and short-wave), and a SEM Jeol JSM 6400 equipped with a Tracor Series II EDX and an Oxford MonoCL 1 system were focused on mineral associations, optical properties, and internal structures of scheelite. The SEM was operated at 20 kV and 0.3 to 1.5 nA beam current.

Trace element contents in scheelite were determined using instrumental neutron activation analyses at the Institute of Nuclear Physics of the Uzbekistan Academy of Sciences (Tashkent) for La, Ce, Eu, Tb, and Lu. Isotope dilution was carried out at the Institute of Precambrian Geology and Geochronology of the Russian Academy of Sciences (St. Petersburg) for determination of Sm, Nd, and Sr.

For isotope analyses, 50–100 mg of powdered scheelite samples were dissolved in 9 N HCl in closed Teflon bombs at 110 °C for at least 24 h. Mixed ^{149}Sm–^{146}Nd and ^{85}Rb–^{84}Sr spikes were added before digestion of the samples. After digestion the solutions were evaporated to dryness on a hot plate and the residues were redissolved in 3 ml of 2.2 N HCl. The samples were heated for 1 h in closed Teflon bombs to ensure the complete removal of the residues into solution. Then the solutions were centrifuged. Further separation of Sm and Nd was carried out according to the standard scheme of two-steps ion-exchange and extraction chromatographic separation (Richard et al. 1976; Amelin et al. 1997). Separation of Rb and Sr was done by cation exchange techniques in 2.2 N HCl media using Bio-Rad 50Wx8, 200–400 mesh resin. Isotope composition and concentrations of Sm, Nd, Rb, and Sr were measured by means of a solid-source 8-collector Finnigan MAT-261 under static mode at the Institute of Precambrian Geology and Geochronology of the Russian Academy of Sciences. The isotope composition of Nd was normalized within-run to a $^{143}Nd/^{144}Nd$ value of 0.511860 for the La Jolla standard. The isotope composition of Sr was normalized to $^{88}Sr/^{86}Sr = 8.37521$. Isotope ratios were measured with precision better than 0.5% for $^{87}Rb/^{86}Sr$, 0.3% for $^{147}Sm/^{144}Nd$, and about 0.5–1.0% for element concentrations (2σ). The blank levels for Sm and Nd were 0.1 and 0.3 ng respectively, as well as 0.05 and 0.7 ng for Rb and Sr. The analytical results obtained on the BCR-1 standard during the course of this work were: [Sm] = 6.43 ppm, [Nd] = 28.2 ppm, $^{147}Sm/^{144}Nd =$

0.13826, $^{143}Nd/^{144}Nd = 0.512655 \pm 7$, [Rb] = 44.6 ppm, [Sr] = 335 ppm, $^{87}Rb/^{86}Sr = 0.38413$, and $^{87}Sr/^{86}Sr = 0.705090 \pm 10$. The isotope ratio $^{87}Sr/^{86}Sr$ for NBS-987 was 0.710239 ± 20 (mean of 15 runs), and the $^{143}Nd/^{144}Nd$ ratio was 0.511894 ± 10 (mean of 9 runs) for the La Jolla standard.

Results

Mineralogical characteristics of scheelite 1 and 2

As mentioned above, two types of scheelite samples have been distinguished according to their geological position, mineralogical properties, and trace element characteristics (Table 1). Scheelite 1 from the flat veins was usually found in small, disseminated grains in greyish quartz. This scheelite type shows signs of strong tectonic deformation (Fig. 4a). Groups of small irregular grains arranged in short trails are probably relics of former larger crystals destroyed by intensive shearing. In some cases, aggregates of up to 1–2 cm in diameter were observed. In such aggregates, the brownish-grey to white coloured and strong bluish-white luminescent scheelite (i.e. Mo-poor with Mo $<<$ 1,000 ppm) is often intergrown with pyrite, pyrrhotite, and K-feldspar. Chlorite, apatite, and calcite were also found.

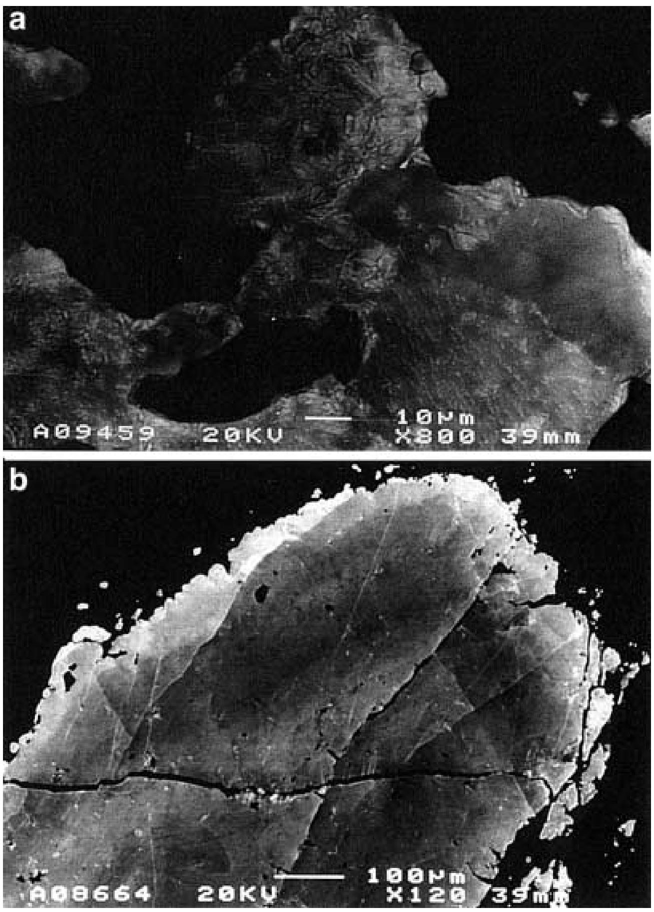

Fig. 4 SEM–CL images (Jeol JSM 6400, 20 kV, 0.6 nA). **a** Internal structure of a strongly deformed grain of scheelite 1 in quartz from a flat vein (sample MT 98–1A). **b** Internal structure of a brecciated crystal of scheelite 2 with broad oscillatory growth zoning (sample MT 1)

Brownish to orange scheelite 2 from steeply dipping veins occurs in aggregates of brecciated crystals up to several centimetres in diameter and as small rounded grains intergrown with milky quartz adjacent to the larger crystals. Scheelite 2 and quartz are cross-cut by later carbonate veinlets. Other minerals found in association with scheelite 2 are muscovite, pyrite, chalcopyrite, molybdenite, and allanite. The internal structure of scheelite 2 revealed by cathodoluminescence (CL) imaging sometimes shows broad oscillatory growth zoning (Fig. 4b). A characteristic feature of scheelite 2 is the quenched yellowish photoluminescence occurring despite very low Mo contents (0.1–2.2 ppm Mo, Kempe, and Oberthür 1996, unpublished). A yellowish tinting is also observable during CL investigation. The decrease of luminescence intensity with increasing intensity of colour found during our study were also mentioned by Uspenskiy and Aleshin (1993). Most probably, this specific feature is due to optically active iron centres and electron defects in the scheelite lattice.

Furthermore, scheelite 1 and 2 may be distinguished by their Sr content (below 300 and above 400 ppm respectively, Table 1) and by the rare earth element (REE) distribution patterns (Fig. 5a). The data reported here for REE in scheelite are slightly different from the results obtained by ICP–MS (Kempe et al. 1999); nevertheless, they have the same main features: Scheelite 1 shows REE distribution patterns similar to the REE distribution patterns of the wall rocks without pronounced Eu anomalies, but with some enrichment of the heavy REE in comparison to the wall rocks. The REE distribution patterns of scheelite 2 are similar to those reported by Anglin et al. (1987) for scheelite from Canadian Au deposits (REE distribution patterns of two selected samples from the Hard Rock and the Sigma mine are shown in Fig. 5b). These patterns are bell-shaped and show positive Eu anomalies. The strong depletion of the heavy REE may be explained by REE fractionation between scheelite and carbonates (Kempe et al. 1999). Summarizing the mineralogical data, we conclude that at least two types of scheelite occur in the Muruntau ore deposit, which may be clearly distinguished not only by their geological position, but also according to their mineralogical–geochemical properties.

Sm–Nd and Rb–Sr isotope data

Isotope results are summarized in Table 3. The Rb contents are very low (generally below 1 ppm; exceptions may be related to traces of micas in the fractions investigated). Compared to the high Sr contents, any in situ produced radiogenic Sr in the scheelite can therefore be neglected. Sr isotope ratios may be used for estimations of the initial Sr isotope composition of the

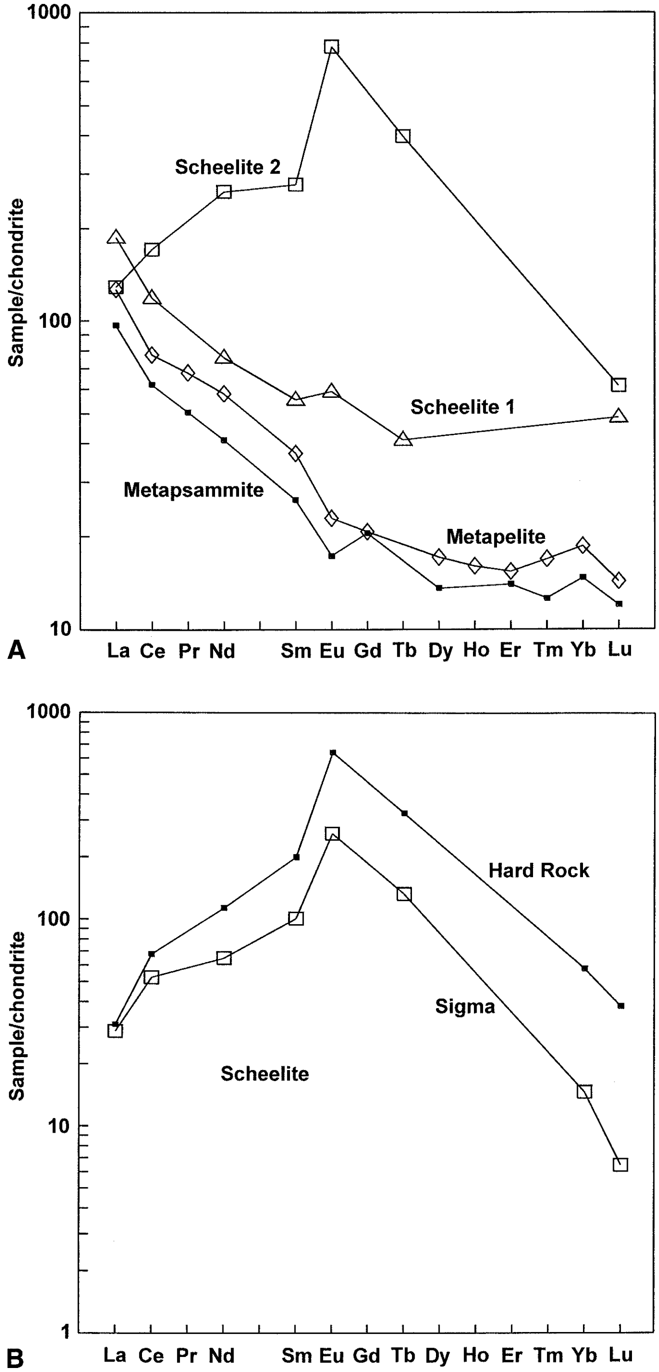

Fig. 5 REE distribution patterns of: **A** scheelite 1 and 2 in comparison with REE patterns of the Muruntau host rocks (averages; data for La, Ce, Eu, Tb, and Lu by INNA; for Sm and Nd by isotope dilution; data for wall rocks from Kremenetsky et al. 1990); **B** two selected scheelite samples from Au deposits in the Timmins area (Canada; data from Anglin et al. 1987)

ore-forming fluid. Initial Sr isotope ratios found for Muruntau, Myutenbai, and Kosmanachi scheelites are rather uniform and range from 0.7146 to 0.7162, with no significant difference between groups 1 and 2.

Samples of scheelite 1 and 2 from Muruntau/Myutenbai plot on two well-defined lines in the Sm–Nd isochron diagram (Fig. 6). Samples of scheelite 1 from flat veins define an apparent age of 351 ± 22 Ma ($\epsilon_{Nd} = -8.4 \pm 0.3$; MSWD: 1.5; Fig. 6a), whereas the isochron for scheelite 2 samples corresponds to an age of 279 ± 18 Ma ($\epsilon_{Nd} = -9.5 \pm 0.3$; MSWD: 1.5; Fig. 6b). The Kosmanachi sample falls below the isochron for scheelite 2. In order to test whether the isochrons are "true" isochrons or represent mixing lines, the $^{143}Nd/^{144}Nd$–1/Nd plot was used (Fig. 7a). Mixing of two components may be assumed if a positive correlation is found between $^{143}Nd/^{144}Nd$ ratio and 1/Nd (or any other parameter that is not directly related to the age). There are no indications for mixing in the case of scheelite 2 (there are some signs of negative correlation), whereas mixing processes may be assumed for scheelite 1 (if sample MT4 is excluded). Since the situation is ambiguous in the case of the $^{143}Nd/^{144}Nd$–1/Nd plot for scheelite 1, we tested additional parameters. As it can be seen from Fig. 7b, there is some correlation between measured $^{143}Nd/^{144}Nd$ ratio and distance to the adjacent ore bodies. Therefore, the regression line in the isotope diagram for scheelite 1 samples may be interpreted as a result of mixing.

Discussion

Applicability of the Sm–Nd isotope system in scheelite for age determination in the Muruntau gold deposit

Absolute age determination using the Sm–Nd isotope system of minerals is possible if (1) initially, there was a fluid system homogeneous in $^{143}Nd/^{144}Nd$ for all investigated samples (starting condition) and if (2) the Sm–Nd system was not disturbed by subsequent alteration processes (boundary condition). Obviously, the starting condition cannot be always fulfilled for quartz vein deposits. As we have shown for the case of Sn–W vein mineralization (Kempe and Belyatsky 1994, 1997, 2000), initial homogenization of the $^{143}Nd/^{144}Nd$ ratios may depend on the homogeneity of the wall rocks. Initial homogenization of the $^{143}Nd/^{144}Nd$ ratios was found in cases where the wall rocks are uniform. In contrast, mixing between two or more Sm–Nd isotope systems is often indicated when different wall rocks are present. In the case of the Muruntau deposit, metasiltstones and metasandstones are rather uniform in their REE characteristics and the granitic rocks represent only a very small portion of the wall rocks. Therefore, we may assume that, in general, the starting condition was probably valid for both investigated scheelite types. Nevertheless, some scatter of the data points around the regression line in the Sm–Nd isochron diagrams can result from remaining heterogeneity in the initial $^{143}Nd/^{144}Nd$ ratios.

The fulfilment of the boundary condition is more difficult to estimate. A weak disturbance of the Sm–Nd isotope system can also cause some scatter of the data points in the isochron diagrams. For scheelite 1, open

Table 3 Sm–Nd and Rb–Sr isotope data for scheelite 1 and 2 from Muruntau, Myutenbai, and Kosmanachi. Initial isotope signatures [ϵ_{Nd}, $(^{87}Sr/^{86}Sr)_i$] are calculated for 350 and 279 Ma for group 1 and 2 respectively. 2σ are measured within-run errors for $^{143}Nd/^{144}Nd$ and $^{87}Sr/^{86}Sr$ isotopic ratios at the 95% confidence level and refer to the last decimal digits

Sample	[Sm] (ppm)	[Nd] (ppm)	$^{147}Sm/^{144}Nd$	$^{143}Nd/^{144}Nd$	2σ	ϵ	[Rb] (ppm)	[Sr] (ppm)	$^{87}Rb/^{86}Sr$	$^{87}Sr/^{86}Sr$	2σ	$(^{87}Sr/^{86}Sr)_i$
Group I scheelite (flat veins)												
MT3773	11.3	30.8	0.22261	0.512273	15	–8.29	0.591	222	0.00770	0.715069	35	0.715031
MT3776	13.8	60.4	0.13869	0.512075	6	–8.40	0.981	219	0.01295	0.714714	17	0.714649
MT3778	13.5	61.0	0.13477	0.512053	7	–8.65	0.151	227	0.00193	0.714975	21	0.714965
MT3779	11.8	39.2	0.18236	0.512165	6	–8.59	2.960	221	0.03900	0.714755	24	0.714561
MT4	5.20	36.6	0.08616	0.511958	6	–8.33	n.d.	n.d.	n.d.	n.d.	–	n.d.
Group II scheelite (steep veins)												
MT1	69.9	194.0	0.21832	0.512193	6	–9.46	0.146	566	0.00075	0.715380	18	0.715377
MT1A	45.4	125.1	0.22011	0.512196	6	–9.46	14.92	825	0.05235	0.715457	14	0.715249
MT2	86.4	223.0	0.23516	0.512210	9	–9.73	1.080	396	0.00792	0.714940	24	0.714909
MT3423	36.2	120.0	0.18189	0.512135	6	–9.29	0.208	963	0.00062	0.715595	20	0.715593
MT76–276	20.1	77.6	0.15699	0.512089	7	–9.30	0.587	1041	0.00163	0.715623	26	0.715617
MT876	27.5	108.0	0.15410	0.512062	6	–9.73	0.994	729	0.00395	0.715116	15	0.715100
Repeat	27.4	107.0	0.15525	0.512060	7	–9.81	0.704	727	0.00281	0.715089	12	0.715078
MT-7	38.2	245.0	0.16914	0.512093	7	–9.66	0.309	636	0.00141	0.714738	24	0.714732
MT3710	86.4	174.2	0.30084	0.512343	6	–9.47	n.d.	n.d.	n.d.	n.d.	–	n.d.
KM80–532	74.6	182.8	0.24755	0.512222	13	–9.93	0.730	819	0.00258	0.716235	19	0.716225

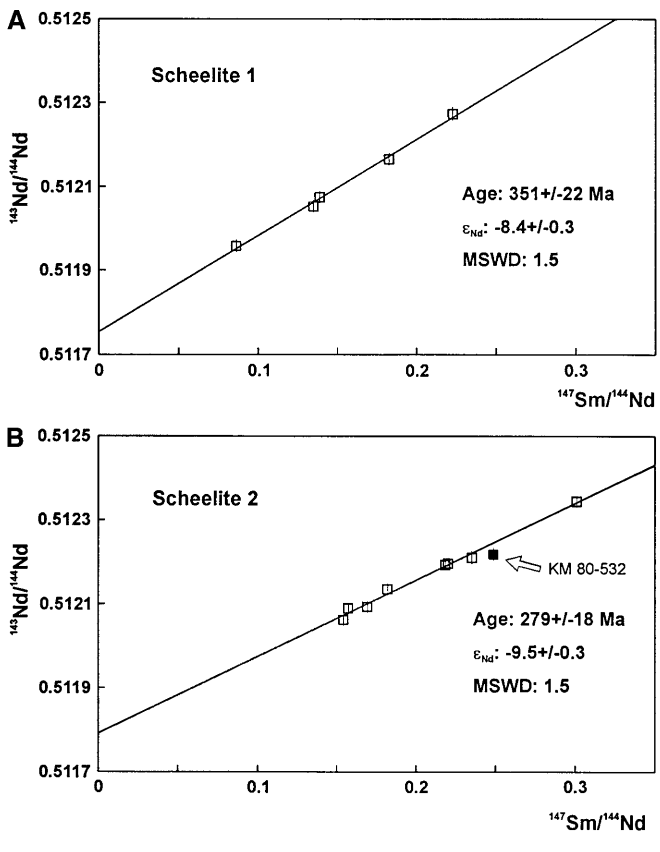

Fig. 6 Sm–Nd isochron plots for scheelite from Muruntau, Myutenbai, and Kosmanachi. **A** scheelite 1; **B** scheelite 2 (sample KM 80–532 was excluded from isochron calculations)

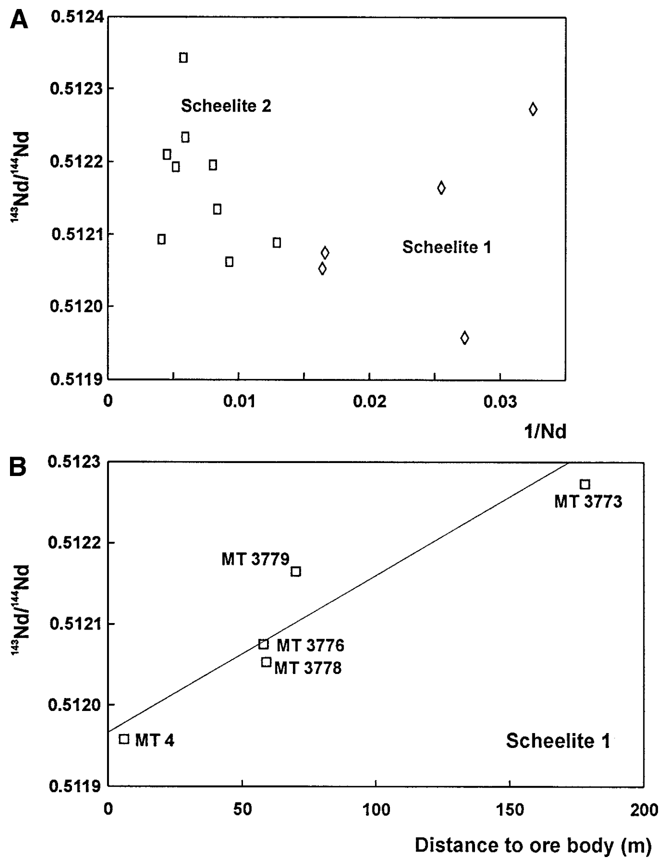

Fig. 7 Tests for mixing lines. **A** $^{143}Nd/^{144}Nd$–1/Nd plots for scheelite 1 and 2. **B** The $^{143}Nd/^{144}Nd$ ratio depends on distance to adjacent ore body for scheelite 1 samples

system behaviour of the Sm–Nd system can be expected (1) from the shear-related deformation of the crystals and/or (2) from fluid circulation during formation of the younger, steeply dipping, and Au-bearing veins with scheelite 2. The importance of the second process can be inferred from the relation between measured $^{143}Nd/^{144}Nd$ ratios of the samples and their distance to the adjacent ore body (Fig. 7b) as well as from fluid inclusion data showing that CO_2-rich inclusions, which are of primary and pseudosecondary origin in steeply dipping quartz veins, are of secondary origin in flat quartz veins (Graupner et al. 1999).

No clear signs were found for disturbance of the Sm–Nd isotope system of scheelite 2, although later processes occurred that may potentially have influenced the Sm–Nd system, such as formation of tourmaline-bearing veins, sulfide veins, and Ag-bearing veins. Only for the scheelite 2 sample from Kosmanachi, where Ag mineralization is developed extensively, is a disturbance of the Sm–Nd system indicated (Fig. 6b).

Sm–Nd isotope data: implications for the absolute age of Au mineralization and related processes

Up to the present, there are no direct age data available for flat and steeply dipping quartz veins in Muruntau/Myutenbai (Table 2). The Rb–Sr systems of the flat and steeply dipping quartz veins were found to be disturbed (Kostitsyn 1991). The Sm–Nd isochron age of 279 ± 18 Ma obtained for scheelite 2 from steeply dipping veins is in good agreement with Rb–Sr mineral (density) isochron ages from Muruntau published by Kostitsyn (1991) for (1) an altered granitic dyke (274 ± 6 Ma), (2) a lamprophyre dyke (sampled in the Tamdytau mountains; 274 ± 5 Ma), (3) biotitized wall rock (273 ± 3 Ma), and (4) feldspatized wall rock (271 ± 17 Ma) as well as with K–Ar ages for biotite, amphibole, and microcline from metasomatically altered rocks (271–277 Ma) and for a lamprophyre (277 ± 5 Ma) reported elsewhere (cf. Table 2). It may be concluded that the steeply dipping high-grade ore bodies including "central" veins, stockworks, and adjacent Au-bearing metasomatically altered rocks were formed at 270–280 Ma. This conclusion is in agreement with suggestions made by Kostitsyn (1996). However, it should be mentioned that, according to our investigations, gold is related to late mineral assemblages including calcite, chlorite, and apatite. If the formation of these assemblages is related to the final stage of quartz-vein formation, then Sm–Nd, Rb–Sr, and K–Ar age data for steeply dipping veins and for minerals from metasomatically altered rocks define the timing of high-grade ore formation at Muruntau and Myutenbai.

The Sm–Nd systematics of scheelite 1 are disturbed and a process of mixing is most probably responsible for the regression line in the Sm–Nd isochron diagram. Therefore, the age defined at 351 ± 22 Ma has no direct geological meaning. Nevertheless, isotope data together with geological observations (boudinage of flat veins, strong shearing and deformation of vein quartz and scheelite), observed internal structures in the vein quartz, and fluid inclusion data (Graupner et al. 1999) lead us to the conclusion that a separate, most probably Caledonian event of low-grade Au–W ore deposition has to be taken into consideration. According to trace element characteristics and mineral association of scheelite 1, a mineralization style similar to that in W–Sb(–Au) deposits can be assumed for this stage (Kempe et al. 1994; Kempe and Oberthür 1997).

At present, the relations between the main hydrothermal event at 270–280 Ma and magmatic processes in the region are poorly constrained. Rb–Sr density isochrons for the Sardarin pluton and a granodioritic dyke (which most probably represent biotite ages; cf. data in Kostitsyn 1996) as well as a Rb–Sr whole rock isochron for the Murun granite (Kostitsyn 1996) suggest an age of around 282–286 Ma for the main granite magmatism in the vicinity of Muruntau. Nevertheless, Rb–Sr data for the Murun granite and the granodioritic dyke have to be interpreted with caution since the extremely low Sr content in the samples from the Murun granite strongly suggests Sr loss. Moreover, the Rb–Sr system in the samples was found to be disturbed (Kostitsyn 1996). Preliminary results of petrographic investigations on rock samples from the Murun granite clearly indicate metasomatic alteration (Kempe et al., unpublished). Data reported by Kostitsyn (1996) show that the carbonate fraction derived from the granodiorite dyke sample also plots on the regression line in the Rb–Sr isochron diagram. The alkaline granite magmatism dated by Kostitsyn (1991) at 274 ± 6 Ma on the basis of a density isochron for a "syenitic" dyke from the drill hole SG 10 cannot be regarded as being well established. Close examination of dyke samples from the ore field revealed that these rocks are strongly altered and the "syenitic" characteristics (particularly the high contents of alkaline feldspar) are most probably a result of potassic alteration. Possibly, Rb–Sr and K–Ar ages found for lamprophyres (274–277 Ma, cf. Table 2) indicate a time overlap of this magmatism with the main stage of ore formation.

Sources of Sr and Nd

The initial Sr isotope values obtained for scheelite 1 and 2 are in good agreement with data reported by Kostitsyn (1996). As discussed by this author, there are no indications for additional sources of Sr besides those of the immediate wall rocks (Fig. 8a). Increased Sr contents in scheelite 1 and 2 are most probably caused by the destruction of Ca-rich (and Sr-rich) plagioclase during wall rock alteration (Kempe and Oberthür 1997). The higher Sr and REE concentrations in scheelite 2 in comparison with scheelite 1 are most probably related to a more intensive wall rock alteration during formation of the steeply dipping vein system. Furthermore, our own results as well as a review of the data reported in the literature show that the Sr content in scheelite from Au quartz-vein deposits clearly depends on the characteristics of the wall rocks. The Sr content of scheelite is high in Au-bearing quartz veins located in rocks containing significant amounts of Ca-rich plagioclase (gabbro, diorite, granodiorite, and metapelite), whereas the Sr content in scheelite is remarkably lower in samples from host rocks with acidic plagioclase or low Ca-rich

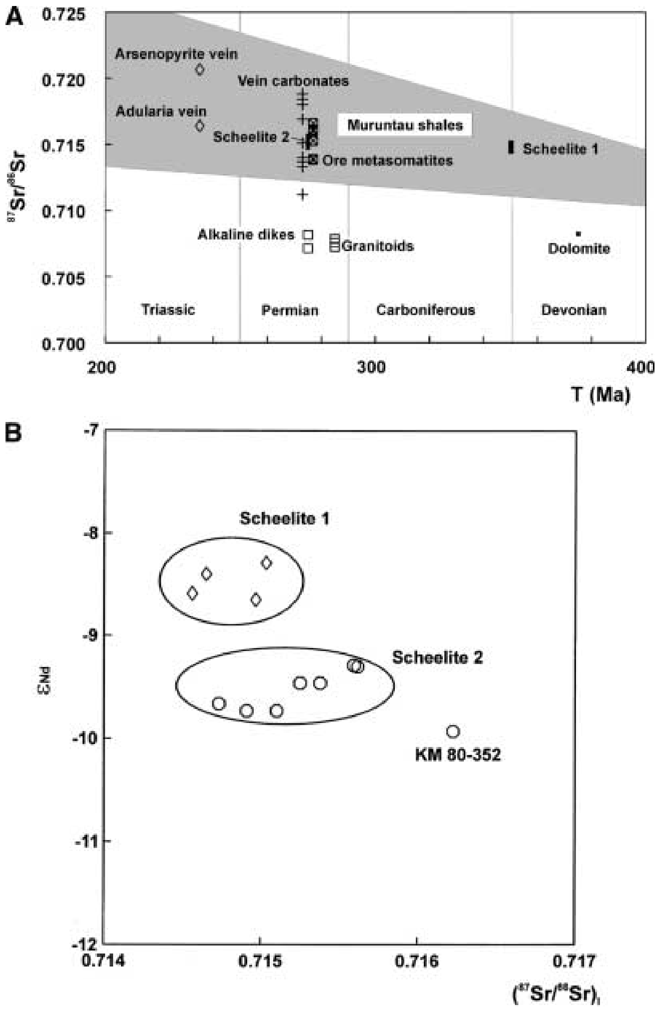

Fig. 8 Nd–Sr signatures of scheelite 1 and 2. **A** Initial Sr of scheelite 1 and 2 in comparison with Sr data for marbles, magmatites, metasomatites, and vein carbonates from Muruntau (according to Kostitsyn 1991). **B** ϵ_{Nd}–$^{87}Sr/^{86}Sr$ diagram for scheelite samples from Muruntau, Myutenbai, and Kosmanachi (ϵ_{Nd} values for scheelite 1 were calculated for a minimal age of 350 Ma as indicated by the isochron calculation; see Table 3 and text for further explanations)

plagioclase contents (basalt, skarn, phyllite, granite; Anglin et al. 1987; Bell et al. 1989; Mueller et al. 1991; Kempe et al. 1994; Oberthür 1995, personal communication; Kempe and Oberthür 1997).

The initial Sr isotope values of the granitic rocks and of the Devonian/Carboniferous marbles are significantly lower than the initial Sr isotope values of the wall rocks, of ore-bearing metasomatically altered rocks, of vein carbonates, and of scheelite 1 and 2 and, therefore, cannot be discussed as a possible Sr source for the ore system (Kostitsyn 1996; Fig. 8a).

ϵ_{Nd} data for scheelite 1 and 2 (Fig. 8b) show that Nd cannot be simply derived from the wall rocks during one event of wall rock alteration, although the low values (averages of –8.4 and –9.5 respectively) clearly indicate crustal signatures. The presence of newly formed REE minerals in the ore veins and metasomatites indicates the mobility of the REE during ore formation. Calculations show that either the Nd was derived from different sources, or there were two discrete (time separated) extractions of Nd from a plagioclase-rich rock (like the wall rocks of Muruntau/Myutenbai). The ϵ_{Nd} data for scheelite support our postulate of two different types of scheelite related to two events of Au(–W) ore formation significantly separated in time. Generally, there is a decrease of ϵ_{Nd} from about –8.4 (calculated for a minimal age of 350 Ma) to –9.5 (calculated for 279 Ma). In addition, the ϵ_{Nd} are higher for scheelite 1 than for scheelite 2 even if the calculations were carried out assuming an identical age for both scheelite types.

Summarizing, we conclude that there are no indications from Sr and Nd isotope data for an influence of external sources on the Au mineralization at Muruntau/Myutenbai. Nevertheless, this statement may not be related to the primary sources of Au and W as already mentioned by Kostitsyn (1996). As we discussed elsewhere (Graupner et al 1999; Kempe et al. 1999) external sources of Au mineralization can be assumed from fluid inclusion as well as mineralogical data. Possibly, the initial Sr and Nd isotope signatures of the ore-forming fluids changed due to intensive fluid–wall rock interaction.

Comparison with scheelite from other gold deposits

Our study as well as data reported in the literature indicate a strong control of the wall rock composition on the Nd and Sr isotope characteristics of scheelite from Au quartz-vein deposits (Fig. 9). Mantle-related wall rocks produce mantle signatures in the Nd–Sr characteristics of the scheelite, whereas crustal rocks give crustal Nd–Sr signatures. As discussed above, this effect is probably due to intensive fluid–wall rock interaction during ore formation. Therefore, the starting condition for Sm–Nd isotope dating (initial homogenization of the $^{143}Nd/^{144}Nd$ ratios) is more easily fulfilled for quartz veins in uniform wall rocks (see also Kempe and Belyatsky 1994, 1997, 2000 for Sn–W deposits).

Conclusions

The Sm–Nd system in scheelite from Au quartz-vein deposits can be used for direct age determination not only in the case of Archean Au mineralization in greenstone belts, but also for deposits in younger geological settings. Correct interpretation of the Sm–Nd and Rb–Sr isotope data requires detailed investigation of both the geological relationships and the mineralogical characteristics of the scheelite samples. More than one generation of scheelite can be present in a single Au quartz deposit.

Two types of scheelite may be clearly distinguished according to their geological relationships, mineralogical characteristics, and isotopic properties in the giant Muruntau/Myutenbai deposit (Uzbekistan). Early,

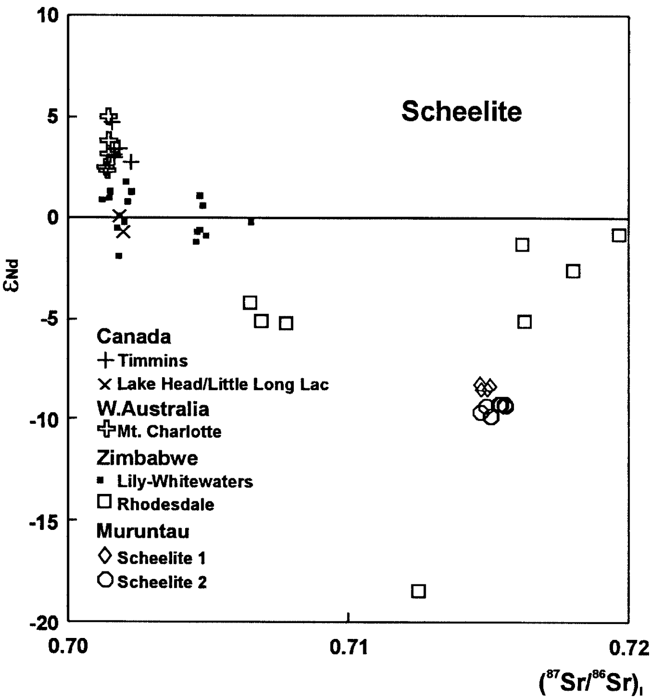

Fig. 9 ϵ_{Nd}–$^{87}Sr/^{86}Sr$ diagram for scheelite samples from Canadian, Australian, African, and Uzbekistan Au deposits illustrating the dependence of the isotope signatures from the wall rocks (data from Bell et al. 1989; Kent et al. 1995; Darbyshire et al. 1996; and this study). Samples from greenstone belts show high ϵ_{Nd} and low initial $^{87}Sr/^{86}Sr$ values. Mantle signatures were found for scheelite from the Mount Charlotte mine, Western Australia, located in a rock suite consisting of komatiites and basalts, as well as for scheelite from the Timmins area in the Abitibi greenstone belt, Canada, sampled from veins hosted by mafic volcanics outside of bodies of quartz porphyries. Crustal signatures with low ϵ_{Nd} and high initial $^{87}Sr/^{86}Sr$ values were obtained for samples from the Rhodesdale granitoid gneiss complex, Zimbabwe, as well as for the samples from Muruntau. Scheelite taken from veins in the Lily–Whitewaters area within the Midlands greenstone belt, Zimbabwe, yields ϵ_{Nd} values close to zero and enhanced initial $^{87}Sr/^{86}Sr$ in accordance with the contrasting characteristics of the wall rocks (Darbyshire et al. 1996)

bluish-white coloured, white to greyish luminescent scheelite 1 from strongly deformed flat quartz veins is related to low-grade Au(–W) mineralization, probably of the W–Sb–Au type. The apparent Sm–Nd isochron age of 351 ± 22 Ma derived from a mixing line has no direct geological meaning. Nevertheless, it could be interpreted as a hint for a separate event of Au mineralization, as supported by the distinct ϵ_{Nd} values of scheelite 1 and 2. Yellowish luminescent, brownish to reddish scheelite 2 from steeply dipping high-grade ore veins defines a Sm–Nd isochron age of 279 ± 18 Ma. This age is interpreted as the age of formation of the high-grade ore bodies (including "central" veins as well as ore-bearing metasomatically altered rocks) and agrees well with Rb–Sr and K–Ar ages for ore-bearing metasomatically altered rocks reported elsewhere. Sr and Nd isotope signatures define the wall rocks as a source for Sr and Nd. Probably, primary fluid signatures changed during intensive fluid–wall rock interaction indicated by intensive hydrothermal alteration. Up to now, there are no reliable hints for any genetic or age relationships between the Au mineralization and the granite magmatism present in the region. The formation of the high-grade ores possibly overlaps in time with the intrusion of lamprophyre dykes.

A review of available data shows a close relationship between wall rock characteristics and Nd–Sr signatures of scheelite from Au quartz vein deposits. These observations are confirmed by scheelites from the Muruntau/Myutenbai deposit.

Acknowledgements The fieldwork in the Muruntau area was kindly supported by A.D. Aksenov. A.P. Aleshin provided us with the scheelite sample MT 3432. His help is greatly appreciated. We are grateful to D. Wolf and L.K. Levsky supporting our analytical work during the course of this study. T. Oberthür, T. Graupner, T. Monecke, and J. Götze are thanked for fruitful discussions on problems of age and genesis of Au deposits. The authors would also like to thank R. Frei and an anonymous reviewer for their useful comments and constructive reviews, which significantly improved the manuscript. We would like to express our special thanks to B. Lehmann for pointing out ways of substantially improving an earlier version of this paper. Fieldwork benefited from a travel grant from the Deutsche Akademische Austauschdienst (DAAD).

References

Akhmedzhanov MA, Coj RV, Korsakov VS, Abduazimova ZM, Borisov OM (1979) Stratigraphic columns of pre-Mesozoic rock sequences in the Central Kyzylkum and adjacent territories (in Russian). Uzb Geol Zh 3:21–25

Amelin YV, Ritsk EY, Neymark LA (1997) Effects of interaction between ultramafic tectonite and mafic magma on Nd–Pb–Sr isotopic systems in the Neoproterozoic Chaya Massif, Baikal–Muya ophiolite belt. Earth Planet Sci Lett 148:299–316

Anglin CD (1990) Preliminary Sm–Nd isotopic analyses of scheelites from Val d'Or gold deposit, Quebec. Curr Res 90–1C:255–259

Anglin CD, Franklin JM, Jonasson IR, Bell K, Hoffman E (1987) Geochemistry of scheelites associated with Archean gold deposits: implications for their direct age determination. Curr Res 87–1A:591–596

Anglin CD, Jonasson IR, Franklin JM (1996) Sm–Nd dating of scheelite and tourmaline: implications for genesis of Archean gold deposits, Val d'Or, Canada. Econ Geol 91:1372–1382

Askarov FA, Bigaeva AR (1965) On the absolute age of magmatic events in the Kyzylkum desert (in Russian). Uzb Geol Zh 4:54–62

Badalova RP, Palej LZ (1965) Principal features of gold mineralisation in Western Uzbekistan (in Russian). Geol Rudn Mestorozhd 7(5):38–46

Bel'kova LN, Ognev VN (1971) Age and origin of gold mineralization of the Muruntau. Dokl Akad Nauk SSSR 197: 100–102

Bell K, Anglin CD, Franklin JM (1989) Sm–Nd and Rb–Sr isotope systematics of scheelite: possible implications for the age and genesis of vein-hosted gold deposits. Geology 17:500–504

Belyatsky BV, Kempe U, Levsky LK (1992) On Sm–Nd ages of wolframites from quartz–wolframite ore deposits in the Erzgebirge, Saxony, Germany (in Russian). Dokl Akad Nauk SSSR 324(3):621–625

Belyatsky BV, Vinogradova LG, Krymsky RSh, Levsky LK (1994) Sm–Nd and Rb–Sr isotope dating of the wolframite – rare metal deposit Zabytoe (in Russian). Petrology 2(3):243–250

Berger BR, Drew LJ, Goldfarb RJ, Snee LW (1994) An epoch of gold riches: the Late Paleozoic in Uzbekistan, central Asia. SEC News 16:1–11

Bojcov VE, Ivanov PA, Min'kin IM (1996) Uranium and gold in the Muruntau deposit (Uzbekistan) (in Russian). In: Litvinenko VS, Smyslov AA, Sokolovskij AK (eds) Unikal'nye mestorozhdenija poleznykh iskopaemykh Rossii – zakonomernosti formirovaniya i razmeshcheniya. Gornij Institut, St Petersburg, pp 50–62

Bukharin AK, Maslennikova IA, Zhuravleva IT, Mambetov AM (1984) The age of Taskazgan and Besapan suits (Lower Paleozoic) in the Kyzyl Kum and similar rocks in the Nuratau (in Russian). Byull Mosk Ova Ispy Prir, Otd Geol 59(3):57–68

Chesley JT, Halliday AN, Scrivener RC (1991) Samarium–neodymium direct dating of fluorite mineralization. Science 252(17):949–951

Corfu F (1993) The evolution of the southern Abitibi greenstone belt in light of precise U–Pb geochronology. Econ Geol 88:1323–1340

Darbyshire DPF, Pitfield PEJ, Campbell SDG (1996) Late Archean and Early Proterozoic gold–tungsten mineralization in the Zimbabwe Archean craton: Rb–Sr and Sm–Nd isotope constraints. Geology 24(1):19–22

Drew LJ, Berger BR, Kurbanov NK (1996) Geology and structural evolution of the Muruntau gold deposit, Kyzylkum Desert, Uzbekistan. Ore Geol Rev 11(2):175–196

Frei R, Nägler TF, Schönberg R, Kramers JD (1998) Re–Os, Sm–Nd, U–Pb, and stepwise lead leaching isotope systematics in shear-zone hosted gold mineralization: genetic tracing and age constraints of crustal hydrothermal activity. Geochim Cosmochim Acta 62(11):1925–1936

Fryer BJ, Taylor RP (1984) Sm–Nd direct dating of the Collins Bay hydrothermal uranium deposit. Geology 12:479–482

Gar'kovec VG (1971) Syngenetic–epigenetic gold deposits of the Kyzylkum type (in Russian). In: Sovremennoe sostoyanie ucheniya o mestorozhdeniyakh poleznykh iskopaemykh. Izd AN UzSSR, Tashkent, pp 53–55 (Abstr)

Gar'kovec VG (1973) Findings of syngenetic–epigenetic deposits of the Kyzylkum type (in Russian). Dokl Akad Nauk SSSR 208(1):163–165

Gar'kovec VG (1975) Lithological and tectonic position of Au mineralisation of the Kyzylkum type (in Russian). Dokl Akad Nauk SSSR 222(1):193–196

Graupner T, Kempe U, Spooner ETC, Bray CJ, Kremenetsky AA (1999) Characterisation of fluids from the giant Muruntau Au-ore field, Uzbekistan, utilizing fluid inclusion microthermometry, volatile and dissolved anion/cation data. In: Stanley CJ, Rankin AH, Bodnar RD et al. (eds) Mineral deposits: processes to processing. Balkema, Rotterdam, pp 37–39

Halliday AN, Shepherd TJ, Dickin AP, Chesley JT (1990) Sm–Nd evidence for the age and origin of a Mississippi Valley Type ore deposit. Nature 344(1):54–56

Kempe U, Belyatsky BV (1994) Sm–Nd ages of wolframites from the Western Erzgebirge–Vogtland region: possible genetic implications. In: Seltmann R, Kämpf H, Möller P (eds) Metallogeny of collisional orogens. Czech Geological Survey, Prague, pp 142–149

Kempe U, Belyatsky BV (1997) An attempt at direct dating of the Sadisdorf Sn–W mineralization, Eastern Erzgebirge (Germany). J Czech Geol Soc 42:21 (Abstr)

Kempe U, Belyatsky BV (2000) Direct isotope dating of W(-Y) mineralization at Kyzyltau (Mongolian Altai): preliminary results. Int Geol Rev 42(5):470–480

Kempe U, Oberthür T (1997) Physical and geochemical characteristics of scheelite from gold deposits: a reconnaissance study. In: Papunen H (ed) Mineral deposits: research and exploration – where do they meet? Balkema, Rotterdam, pp 209–212

Kempe U, Dandar S, Getmanskaya TI, Wolf D (1994) The tungsten–antimony mineralization (focussed on new occurrences in the Mongolian Altai). In: Seltmann R, Kämpf H, Möller P (eds) Metallogeny of collisional orogens. Czech Geol Surv, Prague, pp 301–308

Kempe U, Monecke T, Oberthür T, Kremenetsky AA (1999) Trace elements in scheelite and quartz from the Muruntau/Myutenbai gold deposit, Uzbekistan: constraints on the nature of the ore-forming fluids. In: Stanley et al. (eds) Mineral deposits: processes to processing. Balkema, Rotterdam, pp 373–376

Kent AJR, Campbell IH, McCulloch MT (1995) Sm–Nd systematics of hydrothermal scheelite from the Mount Charlotte mine, Kalgoorlie, Western Australia: an isotopic link between gold mineralization and komatiites. Econ Geol 90:2329–2335

Kerrich R (1991) Radiogenic isotope systems applied to mineral deposits. In: Heaman L, Ludden JN (eds) Short course handbook on applications of radiogenic isotope systems to problems in geology. Mineral Assoc Can, Toronto, pp 365–421

Khamrabaev IK (1958) Magmatic and post-magmatic processes in Western Uzbekistan (in Russian). Akad Nauk UzSSR, Tashkent

Koltsov AB, Kostitsyn YA (1995) Isotopic and thermodynamic model of the Muruntau skarn series (in Russian). Geokhimiya 33(4):512–523

Kostitsyn YA (1991) Rb–Sr systems of rocks and minerals from the Muruntau deposit (in Russian). PhD Thesis, Institute of Geochemistry and Analytical Chemistry of the Soviet Academy of Sciences, Moscow

Kostitsyn YA (1993) Rb–Sr isotope study of the Muruntau deposit. 1. Ore veins dating by the isochrone technique (in Russian). Geokhimiya 31(9):1308–1319

Kostitsyn YA (1994) Rb–Sr isotopic study on the Muruntau deposit: ore-bearing metasomatites (in Russian). Geokhimiya 32(4):486–497

Kostitsyn YA (1996) Rb–Sr isotopic study on the Muruntau deposit: magmatism, metamorphism, and mineralisation (in Russian). Geokhimiya 34(12):1123–1138

Kostitsyn YA, Rusinova OV (1987) Rb–Sr dating of a hydrothermal quartz–adular vein by the isochron method (in Russian). In: Metody izotopnoj geologii, GEOKHI, Moscow, pp 123–125 (Abstr)

Kotov NV, Poritskaya LG (1991) Geological position, mineralogical associations in metasomatites, and genetical aspects of the Au ore deposit Muruntau (Central Kyzylkum) (in Russian). Zap Vses Mineral Oa 120(4):59–69

Kraft M, Kampe A (1994) Rohstoffwirtschaftliche Länderberichte der BGR: XXXVIII Usbekistan. Schweizerbart, Stuttgart

Kremenetsky AA, Lapidus AV, Skryabin VY (1990) Geological and geochemical methods of ore prognosis to the depth (in Russian). Nauka, Moscow

Krymsky RS, Belyatsky BV, Vinogradova LG, Levsky LK (1995) Sm–Nd and Rb–Sr isotope systems of the wolframite–scheelite deposit Rudnoe (Primorie) (in Russian). Petrology 3(4):440–448

Li H, Liu J, Lu HZ (1994) Fluid inclusion Rb–Sr isochron age dating of Xihuashan and Dangping tungsten quartz vein deposits, Jiangxi province, China. In: Abstr 8th Int Conf Geochronology, Cosmology and Isotope Geology, Berkley, p 193 (Abstr)

Marakushev AA, Khokhlov VA (1992) A petrological model for the genesis of the Muruntau gold deposit. Int Geol Rev 34(1):59–76

Mueller AG, deLaeter JR, Groves DI (1991) Strontium isotope systematics of hydrothermal minerals from epigenetic Archean gold deposits in the Yilgarn block, Western Australia. Econ Geol 86:780–809

Mukhin PA, Savchuk YS, Kolesnikov AV (1988) The position of the "Muruntau lens" within the metamorphic rock unit of the Southern Tamdytau (Central Kyzylkum Desert) (in Russian). Geotektonika 2:64–72

Palej LZ, Sher SD (1970) On the absolute age of the gold mineralization in Uzbekistan (in Russian). In: Smirnov VI (ed) Where ore deposits are met. Problems of metallogeny of Tyan-Shan, vol 9, Nauka, Moscow, pp 195–200

Petrovskaya NV (1968) Formation of gold ores in Uzbekistan (in Russian). Geol Rudn Mestorozhd 10(3):3–16

Procenko VF (1990) Metamorphic–metasomatic alteration and gold-ore formation in black shales in Western Uzbekistan (in Russian). Zap Uzb Otd Vses Mineral Oa 43:34–39

Procenko VF, Rubanov AA (1991) Convective–metasomatic rare-metal mineralisation in black shales and granites in Western Uzbekistan (in Russian). In: Barabanov VF (ed) Mineralogiya i geokhimiya vol'framovykh mestorozhdenij. Leningradskij Gosudarstvennyj Universitet, Leningrad, pp 242–251

Rakhmatullaev KR (1980) Different ages for different types of gold ores from the Muruntau ore field (in Russian). Zap Uzb Otd Vses Mineral Oa 33:198–202

Richard P, Schimizu N, Allegre CJ (1976) $^{143}Nd/^{146}Nd$ a natural tracer: an application to oceanic basalts. Earth Planet Sci Lett 31(2):269–278

Savchuk YS, Procenko VF, Kolesnikov AV (1987) Mineral associations in the tectonic structures at Muruntau (in Russian). Zap Uzb Otd Vses Mineral Oa 40:30–33

Shayakubov T, Kremenetsky A, Minzer E, Obraztsov A, Graupner T (1999) The Muruntau ore field. In: Shayakubov T, Islamov F, Kremenetsky A, Seltmann R (eds) Au, Ag, and Cu deposits of Uzbekistan (excursion guidebook), GeoForschungsZentrum, Potsdam, pp 37–74

Spooner ETC (1991) Archean intrusion-hosted, stockwork Au-quartz vein mineralization, Lamaque mine, Val d'Or, Quebec: Part II. Light stable isotope (H, O, C, and S) characteristics and enriched calc-alkaline/shoshonitic igneous geochemistry. In: Robert F, Sheahan P, Green S (eds) Nuna conference on greenstone gold and crustal evolution. Geol Assoc Can, Newfoundland, pp 205–210 (Abstr)

Uspenskiy YI, Aleshin AP (1993) Patterns of scheelite mineralization in the Muruntau gold deposit, Uzbekistan. Int Geol Rev 35:1037–1051

Vikhter BY, Khazan KE, Zarembo YG (1986) Relation between gold and tungsten mineralisation in the Southern Tyan' Shan (in Russian). In: Barabanov VF (ed) Mineralogiya i geokhimiya vol'framovykh mestorozhdenij. Leningradskij Gosudarstvennyj Universitet, Leningrad, pp 307–316

Voronkov AK (1976) Special features of lithology of metamorphic rocks of the Proterozoic Besapan suite in the Central Kyzylkum (in Russian). Uzb Geol Zh 1:70–73

Zarembo YG (1968) Main features of phases of ore formation in the Muruntau deposit (Western Uzbekistan) (in Russian). Voprosy geologii mestorozhdenij zolota i zolotonosnykh rajonov, trudy CNIGRI 79:279–290